Diamond & Related Materials 22 (2012) 82–87

Contents lists available at SciVerse ScienceDirect

Diamond & Related Materials

journal homepage: www.elsevier.com/locate/diamond

Incorporation of single-walled carbon nanotubes with PEDOT/PSS in DMSO for the production of transparent conducting films

Jing Zhang, Lian Gao *, Jing Sun, Yangqiao Liu, Yan Wang, Jiaping Wang

State Key Laboratory of High Performance Ceramics and Superfine Microstructures, Shanghai Institute of Ceramics, Chinese Academy of Sciences, 1295 Dingxi Road, Shanghai 200050, China

ARTICLE INFO

Article history:
Received 29 July 2010
Received in revised form 7 November 2011
Accepted 13 December 2011
Available online 20 December 2011

Keywords:
Carbon nanotube
PEDOT/PSS
Composite
Thin films
Electronic properties
Optical properties

ABSTRACT

Single-walled carbon nanotubes (SWCNTs) were incorporated with poly(3,4-ethylenedioxythiophene)/poly(styrenesulfonate) (PEDOT/PSS) in dimethyl sulfoxide (DMSO) solvent for preparing flexible transparent conducting films on polyethylene terephthalate substrate by using the spray coating method. The best SWCNT-PEDOT/PSS-DMSO film showed high performance with a low sheet resistance of 118 Ω/sq and a high transmittance of 90.5%. The conducting mechanism of SWCNT-PEDOT/PSS-DMSO films was investigated by using both atomic force microscopy and Raman spectroscopy, and the improved performance was attributed to the following: (1) the uniform transparency of SWCNTs across the whole visible light spectrum overcame the undesirable transmittance of PEDOT/PSS films, (2) the conducting SWCNTs instead of insulating excess PSS provided the bridges between the conductive PEDOT/PSS grains, (3) the conductive PEDOT/PSS materials between SWCNT networks reduced the contact resistance between SWCNTs, and (4) the electronic interaction between SWCNTs and PEDOT increased the electronic mobility of the whole films.

1. Introduction

In recent years, transparent conducting films (TCFs) have gained great interest because of their wide applications in electronic devices, such as touch screens, liquid crystal displays, organic light-emitting diodes and photovoltaics [1–6]. The traditional material for TCFs is indium tin oxide (ITO) with excellent conductivity and transparency. However, ITO is easy to crack after repeated use due to its brittle nature [7]. Also it becomes increasingly expensive owing to the shortage of indium in the future [8]. To substitute ITO, much effort has been currently devoted to electrical conductive polymers like poly(3,4-ethylenedioxythiophene)/poly(styrenesulfonate) (PEDOT/PSS) for flexible TCFs [9–14] because of their light weight, high flexibility and stable property [15]. However, some parameters of the conductive polymer based electronic devices do not reach the required value, for instance, the mobility still does not exceed 2 $cm^2 V^{-1} s^{-1}$ [16,17], which limits their application potential. Besides, the transparency of PEDOT/PSS with blue colour is undesirable. It decreases sharply at around 600–800 nm wavelength, which deters its application for TCFs.

Another substituting material for ITO is single-walled carbon nanotubes (SWCNTs), which has been frequently reported as TCFs by many researchers [18–25]. SWCNT films offer good durability and flexibility, ease of processing, low reflectance, natural colour, and stable transparency along the whole visible light spectrum. In addition, the mobility of devices using random SWCNT network films (ca. ~100 $cm^2 V^{-1} s^{-1}$) is much higher than polymer based devices, and the mobility of transistors using aligned arrays of SWCNTs even reaches 2000 $cm^2 V^{-1} s^{-1}$ [8]. Therefore, incorporating SWCNTs with PEDOT/PSS could bring higher performance of flexible TCFs.

To a certain extent, compositing SWCNTs and PEDOT/PSS is able to complement both of their disadvantages. On one hand, the conductive nature of PEDOT/PSS can decrease the contact resistance of tube-tube junctions in SWCNT films [26], and the good chemical and thermal stability of PEDOT/PSS is able to increase the stability of SWCNT films [27]. On the other hand, the advantages of SWCNTs can overcome the disadvantages of PEDOT/PSS films. Firstly, SWCNT films exhibit almost the same transparency across the whole visible light spectrum, which could improve the undesirable transparency of PEDOT/PSS films. Secondly, the high tensile strength [28] and Young's modulus [29] of SWCNTs are able to enhance the mechanical and flexible property of PEDOT/PSS films. Thirdly, the higher electronic mobility [30,31] and lower percolation threshold [32] of SWCNTs can improve the conductivity of the PEDOT/PSS films.

As a matter of fact, the composite of SWCNTs and PEDOT/PSS for TCFs has been investigated by some researchers [33–36]. However, the conductivity of those films still had some distance with that of ITO. Besides, few researchers incorporated SWCNTs with PEDOT/PSS in organic solvents. In our work, SWCNTs were incorporated with PEDOT/PSS in dimethyl sulfoxide (DMSO) for preparing flexible TCFs on polyethylene terephthalate (PET) substrate by the spray coating method. Here, DMSO was used as a dispersant for SWCNTs. Meanwhile,

* Corresponding author. Tel.: +86 21 52412718; fax: +86 21 52413122.
E-mail address: liangao@mail.sic.ac.cn (L. Gao).

0925-9635/$ – see front matter
doi:10.1016/j.diamond.2011.12.008

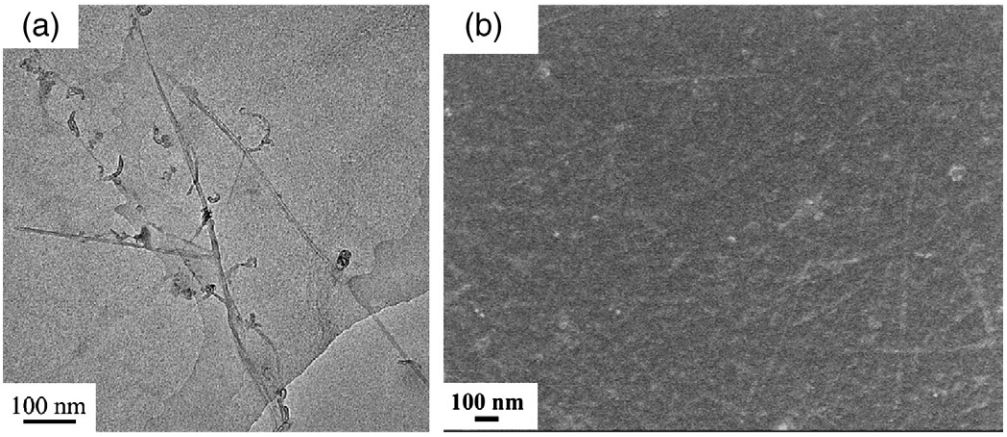

Fig. 1. (a) TEM images of the supernatant of SWCNTs dispersed in DMSO. (b) SEM images of SWCNT-PEDOT/PSS-DMSO films.

DMSO was also able to enhance the conductivity of PEDOT/PSS films 2–3 orders as the secondary dopant [9–11]. Although the origin of the conductivity increase of PEDOT/PSS by secondary dopants was investigated by some researchers, there were still some debates [9–11]. Additionally, conducting mechanism of SWCNT, PEDOT/PSS and DMSO system was seldom investigated systematically before. In this paper, we anatomized the conducting mechanism and the interactions among the three component SWCNTs, PEDOT/PSS and DMSO for the first time by using both atomic force microscopy (AFM) and Raman spectroscopy as analyzing tools, and the improved performance of the SWCNT-PEDOT/PSS-DMSO films was attributed to the following: (1) the conducting SWCNTs instead of insulating excess PSS provided the bridges between the conductive PEDOT/PSS grains, (2) the conductive PEDOT/PSS materials between SWCNT networks reduced the contact resistance between SWCNTs, (3) the interaction between SWCNTs and PEDOT increased the electronic mobility of the whole films.

The best SWCNT-PEDOT/PSS-DMSO film obtained in this work showed sheet resistance of 118 Ω/sq at a transmittance of 90.5% (λ = 550 nm), indicating that the films almost have met the minimum industry standards of applications (100 Ω/sq, 90% T) for substituting ITO [34]. In comparison to the films prepared from SWCNTs and other polymers like Nafion [37] (400 Ω/sq with transmittance of 85% at 550 nm), the properties of our SWCNT-PEDOT/PSS-DMSO films were much more approximate to that of ITO, but more flexible than ITO. Therefore, those SWCNT-PEDOT/PSS-DMSO films are potentially useful as TCFs in flexible transparent electronic devices, such as touch screens, e-papers, displays, transparent transistors, etc.

2. Experimental

The SWCNTs synthesized by chemical vapor deposition (CVD) were obtained from Chengdu Organic Institute. The length of SWCNTs was about 50 μm and the purity of SWCNTs was more than 90 wt.%. To remove metal catalysts, 1.7 g SWCNTs were refluxed in 2.6 M HNO_3 at 140 °C for 48 h. PEDOT/PSS (CLEVIOS PH 500, 1.0–1.3 wt.% solid content) was purchased from H. C. Starck. SWCNT-PEDOT/PSS-DMSO films were prepared by spray coating method on 50 mm × 50 mm PET substrate. 1 mg SWCNTs were firstly dispersed in 10 ml DMSO by bath sonication for 2 h, and then the SWCNT-DMSO solution was centrifuged at 13000 rpm for 30 min. The supernatant was collected and subjected to another round of 30 min centrifugation at 13000 rpm. The final supernatant of SWCNT-DMSO solution was mixed with PEDOT/PSS in volume ratio of 9:1, and bath sonicated for 30 min. Finally, the mixture was sprayed on the PET substrate. A SWCNT-DMSO film and PEDOT/PSS-DMSO (PEDOT/PSS : DMSO = 1:9 in volume) films were also made by the spray coating method to compare with SWCNT-PEDOT/PSS-DMSO films. The obtained films were finally dried at 150 °C for 1 h. Other films were also made with the same procedure as that for SWCNT-PEDOT/PSS-DMSO films, by changing the ratio of SWCNT-DMSO : PEDOT/PSS from 5:1, 15:1 to 19:1.

The morphology of dispersed SWCNTs was observed by transmission electron microscopy (TEM, JEM-2100 F, JEOL, Tokyo, Japan). Images of the films were taken on a field emission scanning electron microscope (FESEM, JEOL, JSM-6700 F). The transmittance of films in visible region was measured by UV–vis spectrometer (Lambda 950, Perkin Elmer, Shelton, U.S.A.). Measurements of the sheet resistances were carried out with a four-point probe resistivity meter (Loresta EP MCP-T360, Mitsubishi Chemical, Japan). The morphology of films was characterized by tapping mode AFM topography and phase images (SPA 400, SPI3800N, Seiko Inc. Japan). Raman spectra of the films were recorded using a MicroRaman spectrometer (LabRam-1B, JY, France) with an excitation length of 633 nm.

3. Results and discussion

Fig. 1a showed the TEM image of SWCNTs dispersed in DMSO for preparing SWCNT-PEDOT/PSS-DMSO films. The bundle sizes were small (10 nm or so), which had positive effect on the conductivity of SWCNT films according to many researches [23,25]. From the SEM image of the SWCNT-PEDOT/PSS-DMSO film shown in Fig. 1b, we found thin bundles of SWCNT networks distributed in the PEDOT/PSS polymer.

Fig. 2 showed the sheet resistance of different films with transmittance at 550 nm. The transmittance was the transparency of the as-prepared conductive films after arithmetically subtracting the transparency of PET substrate. The best SWCNT-PEDOT/PSS-DMSO film in our work had sheet resistance of 118 Ω/sq with a transmittance of 90.5%. Compared with previous reported values for SWCNTs and PEDOT composite films, our films showed better performance. Mustonen et al. [36] prepared films by compositing SWCNTs with PEDOT/PSS in deionized water, and the films had sheet resistance of ~2000 Ω/sq at a transmittance of 80%. Moon et al. [35] incorporated SWCNTs with PEDOT in deionized water for preparing TCFs with the sheet resistance of 247 Ω/sq and transmittance of 84.7%. De et al. [34] dispersed SWCNTs in sodium dodecyl sulfate and then mixed with PEDOT/PSS for preparing films using vacuum filtration method. The films had sheet resistance of ~250 Ω/sq and transmittance of 90%. Wang et al. [33] prepared SWCNT-PEDOT/PSS films by spin coating method, and got films with sheet resistance of ~152 Ω/sq at a transmittance of 83%. Other conductive polymers like Nafion, poly-3-hexylthiophene (P3HT), and poly-3-dodecylthiophene (P3DT) were also used to form composite films with SWCNTs as shown in Fig. 2. For instance, in our previous work [24], SWCNTs were dispersed in Nafion-water/ethanol (water : ethanol = 1:1), and films

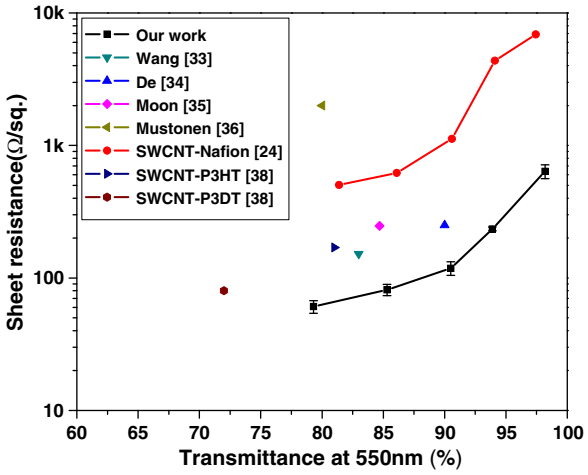

Fig. 2. Sheet resistance versus transmittance at 550 nm for SWCNT-PEDOT/PSS-DMSO films, compared with previously reported literature of SWCNT-PEDOT/PSS films, SWCNT-Nafion films, SWCNT-P3HT films, and SWCNT-P3DT films.

were prepared using the vacuum filtration method. The films with the sheet resistance of 500–600 Ω/sq at transmittance of 85% were obtained. Hellstrom et al. [38] reported that P3HT and P3DT were effectively used to composite with SWCNTs for transparent conducting films. $SOCl_2$ were used to post-treat those films, and sheet resistance of 170 Ω/sq at 81% transmittance for SWCNT-P3HT films and sheet resistance of 80 Ω/sq at 72% transmittance for SWCNT-P3DT films were obtained. In comparison to those previous literatures, our results were better than others. One reason was that SWCNT-DMSO : PEDOT/PSS with appropriate ratio was used, where DMSO not only acted as a dispersant for SWCNTs but also as a secondary dopant to increase the conductivity of PEDOT/PSS films. The performances of films with different proportions of SWCNT-DMSO : PEDOT/PSS were shown in Fig. S1 in supplementary material, and the best performance was obtained when the ratio of SWCNT-DMSO and PEDOT is 9:1.

Without considering the factor of transmittance, the sheet resistance of all the SWCNT-PEDOT/PSS-DMSO (SWCNT-DMSO : PEDOT/PSS = 9:1) films was found to be lower than that of PEDOT/PSS-DMSO (DMSO : PEDOT/PSS = 9:1) films at the same volume of the mixtures which were used for preparing films, as shown in Fig. 3, indicating that SWCNTs had positive effect on decreasing the sheet resistance of PEDOT/PSS-DMSO films. For the same level of conductivity, SWCNT-PEDOT/PSS-DMSO films showed a small variation in transmittance of 3% in the whole visible region, while the variation of the PEDOT/PSS-DMSO films is 7%, as shown in Fig. 4, which meant that SWCNTs had positive effect on the transmittance of PEDOT/PSS films in the visible spectrum. The conducting mechanism and the interactions among SWCNTs, PEDOT/PSS and DMSO will be discussed in the following part according to the AFM and Raman spectra.

The morphology of different films was characterized by tapping-mode AFM. For the SWCNT-DMSO film, the small nanotube bundles can be visualized as shown in Fig. 5a and c, corresponding to the dark areas in the phase images as shown in Fig. 5b and d. The topography of PEDOT/PSS-DMSO film was shown in Fig. 5e and g, and particles with some elongated features were observed. Fig. 5f and h showed the corresponding phase images of PEDOT/PSS-DMSO film, for which the bright areas were identified as conducting PEDOT/PSS domains, while the darker areas were the insulating excess PSS material [9,39]. For PEDOT/PSS films without secondary dopants, the conducting PEDOT/PSS particles were covered with the insulating PSS thin layer and blended in a PSS matrix, according to Crispin et al. [9]. Thus, the conductive PEDOT/PSS particles do not connect well with each other, making the whole film have lower conductivity. In our case, after addition of the secondary dopant DMSO, the excess PSS was phase-segregated into insulating domains, as shown in Fig. 5 e,f,g,h, which was very similar to the effect of diethylene glycol (DEG) [9]. Thus the highly conductive PEDOT/PSS particles merged together to form a three-dimensional conducting network, and significantly improved the conductivity of the whole film.

For the AFM images of SWCNT-PEDOT/PSS-DMSO films (as shown in Fig. 5 i,j,k,l), small bundles of SWCNTs were observed in the PEDOT/PSS polymer matrix. The conducting SWCNTs instead of insulating excess PSS provided the bridges between the conductive PEDOT/PSS grains, resulting in higher conductivity of the whole films. From the other point of view, there were conductive PEDOT/PSS materials between SWCNT networks, which reduced the contact resistance between SWCNTs. That explained why after SWCNTs were incorporated with PEDOT/PSS in DMSO, the sheet resistance of films became smaller than that of PEDOT/PSS-DMSO films from the macroscopic level.

Fig. 6 showed the Raman spectra of different films. For PET substrate (Fig. 6o), there were two main peaks at around 1290 cm^{-1} and 1615 cm^{-1}. Therefore, those two main peaks were also observed for SWCNT-DMSO film (Fig. 6b) and SWCNT- PEDOT/PSS-DMSO film (Fig. 6e). For SWCNT powders, the G band located at 1581.5 cm^{-1}, as shown in Fig. 6a. After SWCNTs were dispersed in DMSO and

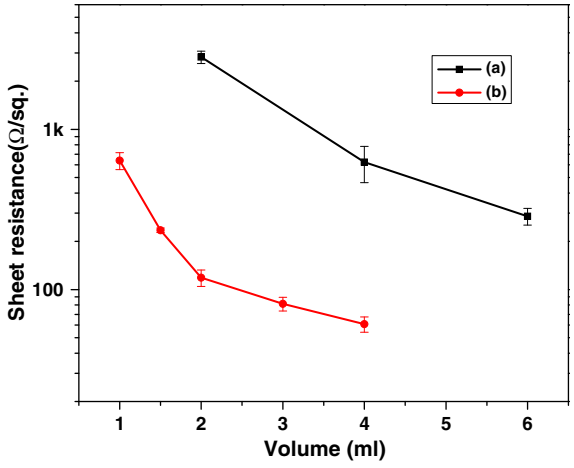

Fig. 3. The sheet resistance of (a) PEDOT/PSS-DMSO (DMSO:PEDOT/PSS = 9:1) films and (b) SWCNT-PEDOT/PSS-DMSO (SWCNT-DMSO:PEDOT/PSS = 9:1) films versus the volume of the mixtures for preparing films.

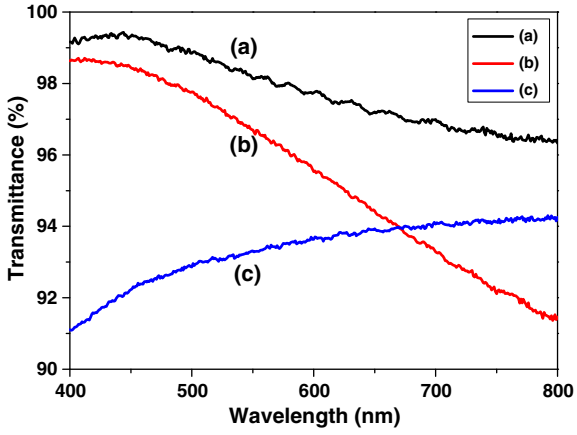

Fig. 4. The transmittance in the visible spectrum of (a) SWCNT-PEDOT/PSS-DMSO film, sheet resistance: 637 Ω/sq, (b) PEDOT/PSS-DMSO film, sheet resistance: 623 Ω/sq, (c) SWCNT-DMSO film.

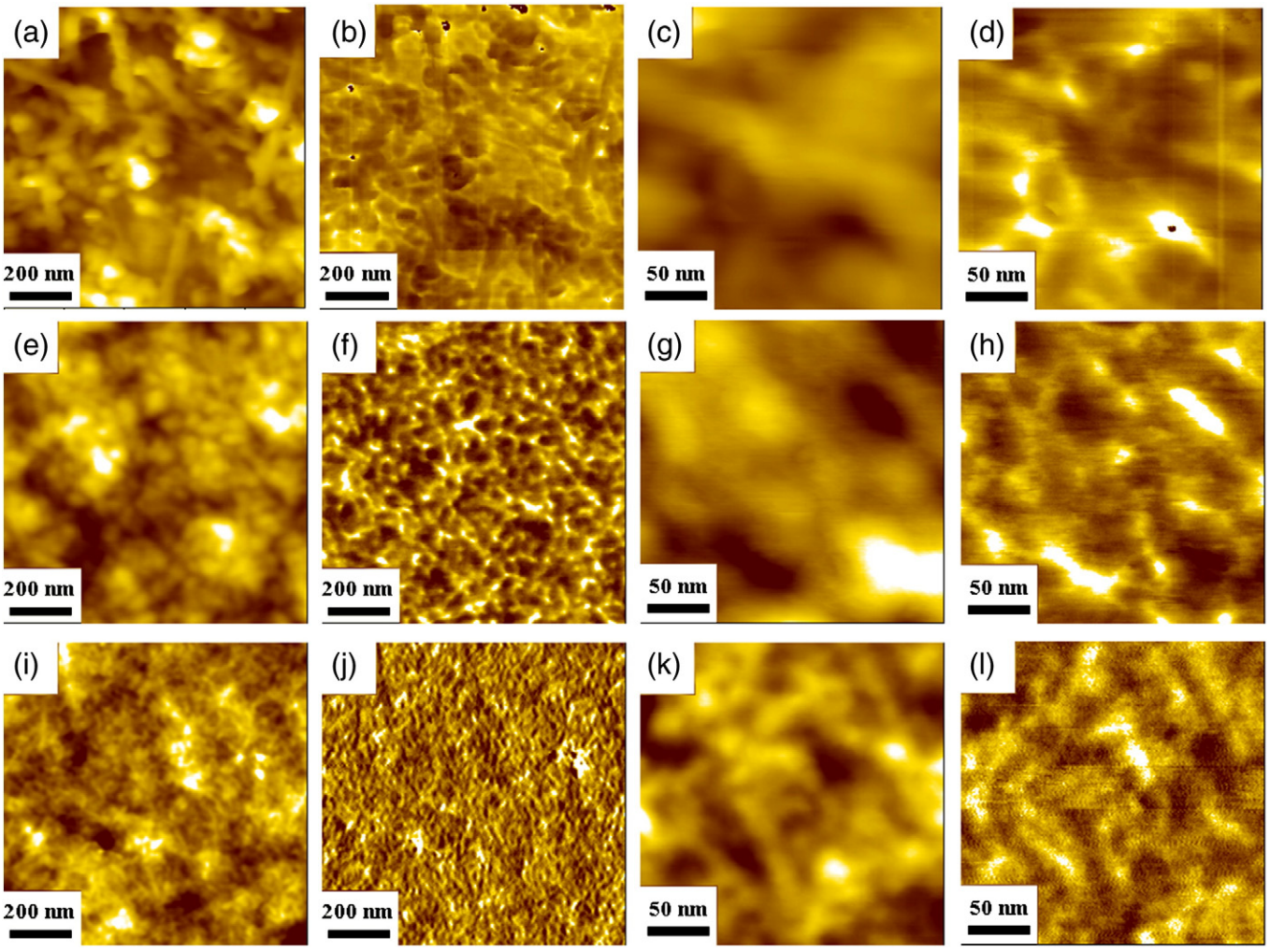

Fig. 5. Topography (a,c,e,g,i,k) and phase images (b,d,f,h,j,l) of a SWCNT-DMSO film(a,b,c,d), a PEDOT/PSS-DMSO film (e,f,g,h), and a SWCNT-PEDOT/PSS-DMSO film (i,j,k,l) with tapping-mode AFM at a scale of 1×1 and 0.25×0.25 μm^2.

sprayed on the PET substrate, the G band of the SWCNT-DMSO film (Fig. 6b) up-shifted by 6.1 cm^{-1}. According to previous reports, the G band of Raman spectra was shifted to the higher frequency (blue shift) by p-doping (like bromine [40] as electron-acceptor) or oxidizing (like by HNO_3 [41] or H_2SO_4 [42]). In our case, the blue shift of the SWCNT-DMSO film might be due to the electronegativity of S atom on the DMSO, resulting in the p-doped SWCNTs.

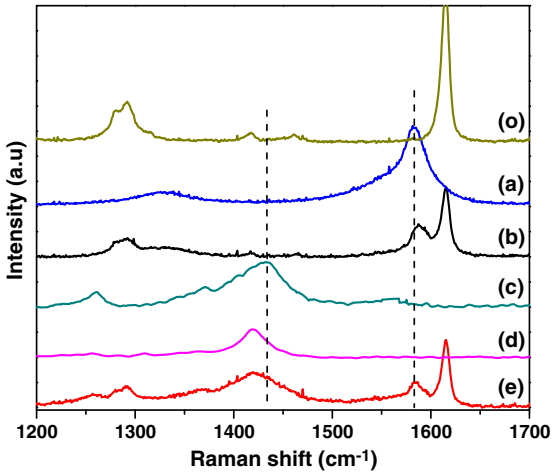

Fig. 6. Raman spectra taken at 633 nm: (o) PET substrate, (a) SWCNT powders, (b) SWCNT-DMSO film, (c) PEDOT/PSS liquid, (d) PEDOT/PSS-DMSO liquid, and (e) SWCNT-PEDOT/PSS-DMSO film.

For the PEDOT/PSS liquid (Fig. 6c), there was a peak at 1436 cm^{-1}, which was assigned to the $C_\alpha=C_\beta$ symmetric vibration for the five-member thiophene ring on the PEDOT chains [43,44]. This $C_\alpha=C_\beta$ peak was reported to red-shift when the thiophene ring presented in PEDOT/PSS changed from benzoid structure to more conductive quinoid structure [44], and meanwhile the conformation of PEDOT chains changed from coil to expanded-coil or linear conformations [11,12]. In our case, after DMSO was added to PEDOT/PSS, the symmetric $C_\alpha=C_\beta$ peak was red-shifted 8.1 cm^{-1}, as shown in Fig. 6d, which was similar to ethylene glycol (EG) [11] and meso-erythritol (E) [12] doped PEDOT/PSS. Thus, after the structure changed from benzoid to quinoid, the neighboring thiophene rings in the PEDOT chains were almost in the same plane, and the conjugated π-electrons could be delocalized over the whole chain according to Ouyang et al. [12], resulting in more conductive PEDOT.

Compared with the PEDOT/PSS liquid, the $C_\alpha=C_\beta$ symmetric peak of SWCNT-PEDOT/PSS-DMSO film was downshifted 9 cm^{-1}, indicating that SWCNT-DMSO also made the structure of PEDOT change from benzoid to the quinoid. However, compared with the PEDOT/PSS-DMSO liquid, there was a broad shoulder at higher frequency for the Cα = Cβ symmetric band of SWCNT-PEDOT/PSS-DMSO film, indicating that only small part of benzoid structure wasn't transformed into the quinoid structure. Besides, the G-band of SWCNT-

PEDOT/PSS-DMSO films was upshifted 5.2 cm^{-1} in comparison to SWCNT powders, and downshifted 0.9 cm^{-1} compared with that of SWCNT-DMSO film, indicating that SWCNT-DMSO were n-doped by PEDOT. The conducting mechanism was interpreted in the following part. For SWCNT-PEDOT/PSS-DMSO films, the SWCNTs were firstly dispersed in DMSO, and the supernatant SWCNTs were easily p-doped by DMSO according to the Raman spectrum of the SWCNT-DMSO film. After the supernatant was mixed with PEDOT/PSS, the two polar dipoles (SO and SCH_3) [12] of DMSO interacted with PEDOT, and made the conformation of PEDOT change from the benzoid to the quinoid structure. Then the delocalized π-electrons over PEDOT chains interacted with SWCNTs. Since SWCNTs were firstly p-doped by DMSO, the conjugated π-electrons over PEDOT chains were easily shifted to SWCNTs. The charge transfer between SWCNTs and PEDOT could increase the conductivity of the whole films, which explained why the sheet resistance of SWCNT-PEDOT/PSS-DMSO films was smaller than that of PEDOT/PSS-DMSO films.

Based on the analysis of Raman spectra, we charted the conformation of PEDOT/PSS, PEDOT/PSS-DMSO and SWCNT-PEDOT/PSS-DMSO films, as shown in Fig. 7. For PEDOT/PSS films, most of the conformation of PEDOT was coil, and the favored structure was the benzoid structure, resulting in worse conductivity of films. After addition of DMSO to PEDOT/PSS, the conformation of PEDOT changed from coil to the expanded coil or linear, and the favored structure became more conductive quinoid structure, resulting in the improvement of conductivity for PEDOT/PSS-DMSO films. For SWCNT-PEDOT/PSS-DMSO films, most of the benzoid structure transformed into quinoid structure, and the favored conformation became expanded coil or linear for PEDOT. In this case, most part of π-electrons delocalized over PEDOT chains, and the electronic interaction between PEDOT and SWCNTs became strong.

From the schematic conformation of different films (Fig. 7), it seemed that the PEDOT/PSS-DMSO system had more contribution to the conformation of PEDOT transformation from benzoid structure to the more conductive quinoid structures than SWCNT-PEDOT/PSS-DMSO system did. However, the conductivity of PEDOT/PSS-DMSO films was still worse than that of SWCNT-PEDOT/PSS-DMSO films. There were three reasons to explain this. Firstly, the SWCNTs instead of insulating excess PSS provided the bridges between the conductive PEDOT/PSS grains, resulting in higher conductivity of the whole films. Secondly, there were conductive PEDOT/PSS materials between SWCNT networks, which reduced the contact resistance between SWCNTs. Thirdly, the interaction between SWCNTs and PEDOT increased the electronic mobility of the whole films, resulting in the improved conductivity of SWCNT-PEDOT/PSS-DMSO films.

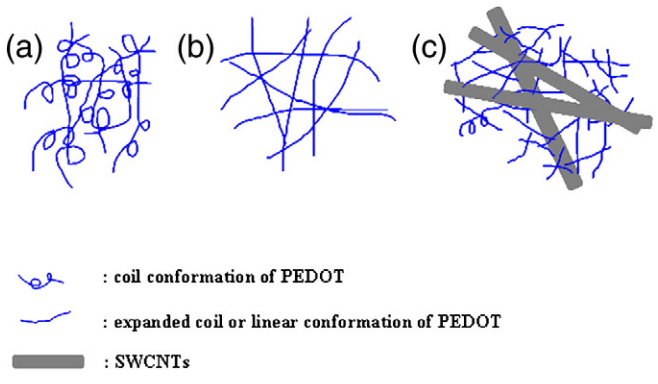

Fig. 7. Schematic conformation of (a) PEDOT/PSS film, (b) PEDOT/PSS-DMSO film, and (c) SWCNT-PEDOT/PSS-DMSO film.

4. Conclusions

Our research indicated that the composite of SWCNTs and PEDOT/PSS in DMSO solvent provided a useful and effective avenue for preparing flexible TCFs with high performance. The uniform transparency of SWCNTs across the whole visible light spectrum overcame the undesirable transmittance of PEDOT/PSS films, resulting in the less transmittance variation of the SWCNT-PEDOT/PSS-DMSO films. The enhanced conductivity of SWCNT-PEDOT/PSS-DMSO films was attributed to the synergistic interaction between the two components: SWCNTs and PEDOT/PSS. From the macroscopic level, the existence of SWCNTs (instead of insulting excess PSS) made the conductive PEDOT/PSS domains connected better. At the same time, the existence of conductive polymer PEDOT effectively decreased the contact resistance between bundles of the SWCNT network, according to the AFM. From microscopic level, the electronic interaction between SWCNTs and PEDOT made SWCNTs doped, and improved the electronic mobility of SWCNT-PEDOT/PSS-DMSO films, according to the Raman spectra. The SWCNT-PEDOT/PSS-DMSO films showed the best performance with sheet resistance of 118 Ω/sq at a transmittance (at $\lambda = 550$ nm) of 90.5%, suggesting that they are promising candidates for replacing ITO in flexible electronic devices, such as touch screens, e-papers, flexible displays, etc.

Acknowledgments

This work was supported by the National Key Basic Research Development Program of China (2005CB623605), the Shanghai Rising-Star Program (08QA14073), the Shanghai Talents Program Foundation, and the Shanghai Institute of Ceramics (SCX200709).

Appendix A. Supplementary data

Supplementary data to this article can be found online at doi:10.1016/j.diamond.2011.12.008.

References

[1] D.L. Carroll, R. Czerw, S. Webster, Synth. Met. 155 (2005) 694.
[2] J. Herrero, C. Guill, Vacuum 67 (2002) 611.
[3] H. Hosono, H. Ohta, M. Orita, K. Ueda, M. Hirano, Vacuum 66 (2002) 419.
[4] L. Wei, Q. Chen, Y.J. Gu, J. Alloys Compd. 501 (2010) 313.
[5] A.A. Dakhel, J. Alloys Compd. 470 (2009) 195.
[6] T. Izumi, K. Izumi, N. Kuroiwa, A. Senjuh, A. Fujimoto, M. Adachi, T. Yamamoto, J. Alloys Compd. 480 (2009) 123.
[7] Y. Leterrier, L. Medico, F. Demarco, J.A.E. Manson, U. Betz, M.F. Escola, M. Kharrazi Olsson, F. Atamny, Thin Solid Films 460 (2004) 156.
[8] Q. Cao, J.A. Rogers, Adv. Mater. 21 (2009) 29.
[9] X. Crispin, F.L.E. Jakobsson, A. Crispin, P.C.M. Grim, P. Andersson, A. Volodin, C. van Haesendonck, M. Van der Auweraer, W.R. Salaneck, M. Berggren, Chem. Mater. 18 (2006) 4354.
[10] J.Y. Kim, J.H. Jung, D.E. Lee, J. Joo, Synth. Met. 126 (2002) 311.
[11] J. Ouyang, Q.F. Xu, C.-W. Chu, Y. Yang, G. Li, J. Shinar, Polymer 45 (2004) 8443.
[12] J. Ouyang, C.-W. Chu, F.-C. Chen, Q.F. Xu, Y. Yang, Adv. Funct. Mater. 15 (2005) 203.
[13] H.T. Ham, Y.S. Choi, M.G. Chee, M.H. Cha, I.J. Chung, Polym. Eng. Sci. 48 (2008) 1.
[14] B. Wessling, Synth. Met. 135–136 (2003) 265.
[15] R.H. Friend, R.W. Gymer, A.B. Holmes, J.H. Burroughes, R.N. Marks, C. Taliani, D.D.C. Bradley, D.A.D. Santos, J.L. Bredas, M. Logdlund, W.R. Salaneck, Nature 397 (1999) 121.
[16] A.R. Brown, A. Pomp, C.M. Hart, D.M. de Leeuw, Science 270 (1995) 972.
[17] Y. Chen, J. Au, P. Kazlas, A. Ritenour, H. Gates, M. McCreary, Nature 423 (2003) 136.
[18] Z.C. Wu, Z.H. Chen, X. Du, J.M. Logan, J. Sippel, M. Nikolou, K. Kamaras, J.R. Reynolds, D.B. Tanner, A.F. Hebard, A.G. Rinzler, Science 305 (2004) 1273.
[19] Y.X. Zhou, L.B. Hu, G. Gruner, Appl. Phys. Lett. 88 (2006) 123109.
[20] M.A. Meitl, Y.X. Zhou, A. Gaur, S. Jeon, M.L. Usrey, M.S. Strano, J.A. Rogers, Nano Lett. 4 (2004) 1643.
[21] D.H. Zhang, K.M. Ryu, X.L. Liu, E. Polikarpov, J. Ly, M.E. Tompson, C.W. Zhou, Nano Lett. 6 (2006) 1880.
[22] E. Artukovic, M. Kaempgen, D.S. Hecht, S. Roth, G. Gruner, Nano Lett. 5 (2005) 757.
[23] G. Gruner, J. Mater. Chem. 16 (2006) 3533.
[24] J. Zhang, L. Gao, J. Sun, Y.Q. Liu, Y. Wang, J.P. Wang, H. Kajiura, Y.M. Li, K. Noda, J. Phys. Chem. C 112 (2008) 16370.

[25] H.-Z. Geng, K.K. Kim, K.P. So, Y.S. Lee, Y. Chang, Y.H. Lee, J. Am. Chem. Soc. 129 (2007) 7758.
[26] G.Z. Xiao, Y. Tao, J.P. Lu, Z.Y. Zhang, Thin Solid Films 518 (2010) 2822–2824.
[27] R. Jackson, B. Domercq, R. Jain, B. Kippelen, S. Graham, Adv. Funct. Mater. 18 (2008) 2548.
[28] F. Li, H.M. Cheng, S. Bai, G. Su, M.S. Dresselhaus, Appl. Phys. Lett. 77 (2000) 3161.
[29] J.-P. Salvetat, G.A. Briggs, J.-M. Bonard, R.R. Bacsa, A.J. Kulik, T. Stockli, N.A. Burnham, L. Forro, Phys. Rev. Lett. 82 (1999) 944.
[30] I. Singh, P.K. Bhatnagar, P.C. Mathur, I. Kaur, L.M. Bharadwaj, R. Pandey, Carbon 46 (2008) 1141.
[31] S. Hong, S. Myung, Nat. Nanotechnol. 2 (2007) 207.
[32] L. Hu, D.S. Hecht, G. Gruner, Nano Lett. 4 (2004) 2513.
[33] G.-F. Wang, X.-M. Tao, R.-X. Wang, Nanotechnology 19 (2008) 145201.
[34] S. De, P.E. Lyons, S. Sorel, E.M. Doherty, P.J. King, W.J. Blau, P.N. Nirmalraj, J.J. Boland, V. Scardaci, J. Joimel, J.N. Coleman, ACS Nano 3 (2009) 714.
[35] J.S. Moon, J.H. Park, T.Y. Lee, Y.W. Kim, J.B. Yoo, C.Y. Park, J.M. Kim, K.W. Jin, Diamond Relat. Mater. 14 (2005) 1882.
[36] T. Mustonen, K. Kordas, S. Saukko, G. Toth, J.S. Penttila, P. Helisto, H. Seppa, H. Jantunen, Phys. Status Solidi B 244 (2007) 4336.
[37] H.-Z. Geng, K.K. Kim, C. Song, N.T. Xuyen, S.M. Kim, K.A. Park, D.S. Lee, K.H. An, Y.S. Lee, Y. Chang, Y.J. Lee, J.Y. Choi, A. Benayad, Y.H. Lee, J. Mater. Chem. 18 (2008) 1261.
[38] S.L. Hellstrom, H.W. Lee, Z. Bao, ACS Nano 3 (2009) 1423.
[39] Y. Wang, R. Song, Y.S. Li, J.S. Shen, Surf. Sci. 530 (2003) 136.
[40] A.M. Rao, P.C. Eklund, S. Bandow, A. Thess, R.E. Smalley, Nature 388 (1997) 257.
[41] U.J. Kim, C.A. Furtado, X. Liu, G. Chen, P.C. Eklund, J. Am. Chem. Soc. 127 (2005) 15437.
[42] C. Engtrakul, M.F. Davis, T. Gennett, A.C. Dillon, K.M. Jones, M.J. Heben, J. Am. Chem. Soc. 127 (2005) 17548.
[43] S. Garreau, J.L. Duvail, G. Louarn, Synth. Met. 125 (2002) 325.
[44] M. Lapkowski, A. Pron, Synth. Met. 110 (2000) 79.